Mechanical behavior of materials in manufacturing processes with material separation

João Pedro Rodrigues Cardoso

Abstract

In metal forming processes, the identification of material flow curve at the appropriate rates of loading is one of the most important parameter for achieving a more realistic modelling of the manufacturing process. However, a brief bibliographical review shows that there are certain disagreements. As the following, this work presents an experimental study to identify and explain some of these discrepancies.
The evolution of the flow stress of the aluminium alloy AA 1050 is presented at different strain and strain rate, taking into account the typical velocity evolution of different manufacturing processes, such as blanking and metal cutting. The experiments were conducted in an innovative cam-driven electromagnetic test machine at high strain rates, which allows to reproduces the typical velocity evolution for several manufacturing processes. The present study also focused on separation processes such as blanking and metal cutting, from the view of ductile fracture mechanics, where the key parameters, such as, the maximum load and normal stress were evaluated. Input parameters such as the flow stress and the fracture toughness, were utilized in a finite element analysis software (I-FORM) for modelling the separation mechanism, which marks the blanking and metal cutting processes.

Keywords Mechanical behaviour of materials, Flow stress, Fracture toughness, Blanking, Orthogonal metal cutting

1. Introduction

The mechanical behavior of the material is an input parameter of great importance for the modelling of metal forming processes for industrial applications (for the project of tools and dies and the selection of machine-tools) and for the research works directed for the comprehension of the fundamentals of the manufacturing processes. However, despite the apparent success of the experimental tests have demonstrated for quantifying the input parameters for metal forming processes, there are some processes where there lacks an universal agreement. Discrepancies between the theoretical models and experiments were pointed out by several authors (Tekkaya, 2009; Atkins, 2000), only seem to indicate that a review of the quantification method of these input parameters should be taken into account.
In this context, this work is focused on the importance of ductile fracture mechanics in manufacturing processes with material separation, such as blanking and metal cutting, where the key parameters, such as, the maximum load and normal stress were evaluated.
The flow curve at the appropriate rates of loading is very important to describe the hardening behaviour during plastic deformation in terms of strain, strain-rate and temperature, to set-up the non-linear constitutive equations of metal plasticity and to establish the feasibility window and effectiveness of manufacturing processes. However, despite this importance, the flow curve is not always accessible in conditions similar to real manufacturing due to difficulties in replicating the operative conditions, namely the combined evolution and range of strains and strain-rates.
In case of strain-rates, for example, the widely available universal testing machines can only perform mechanical characterization of materials at quasi-static or low rate loading conditions ($\dot{\bar{\varepsilon}}$ ~10^{-3} to 1 s^{-1}) and commercially available drop weight testing systems are only adequate for medium rates of loading ($\dot{\bar{\varepsilon}}$ ~1 to 10^3 s^{-1}). Special purpose testing equipment based on split Hopkinson pressure bars, which is adequate for high rates of loading ($\dot{\bar{\varepsilon}} > 10^3$ s^{-1}), and Taylor impact or shock loading by plate impact systems, which are necessary for even higher rates of loading ($\dot{\bar{\varepsilon}} > 10^4$ s^{-1}), are not readily available or guaranteed to the majority of researchers.
However, even if equipment for testing at high rates of loading is available, a frequently ignored and mismanaged technical issue is the adequacy of testing conditions to the operational settings of the machine-tools where manufacturing processes will take place. In fact, despite theoretical claims on transferability of results often requiring mechanical testing of materials with different strain and strain-rate loading profiles to provide the same stress response for a given value of strain and strain rate, it is known that the flow curves obtained under different testing conditions do not coincide for the same material [1]. Not only time history of strain and strain-rate influences stress response [2] as it is relevant to determine crystallographic textures resulting from manufacturing processes [3].

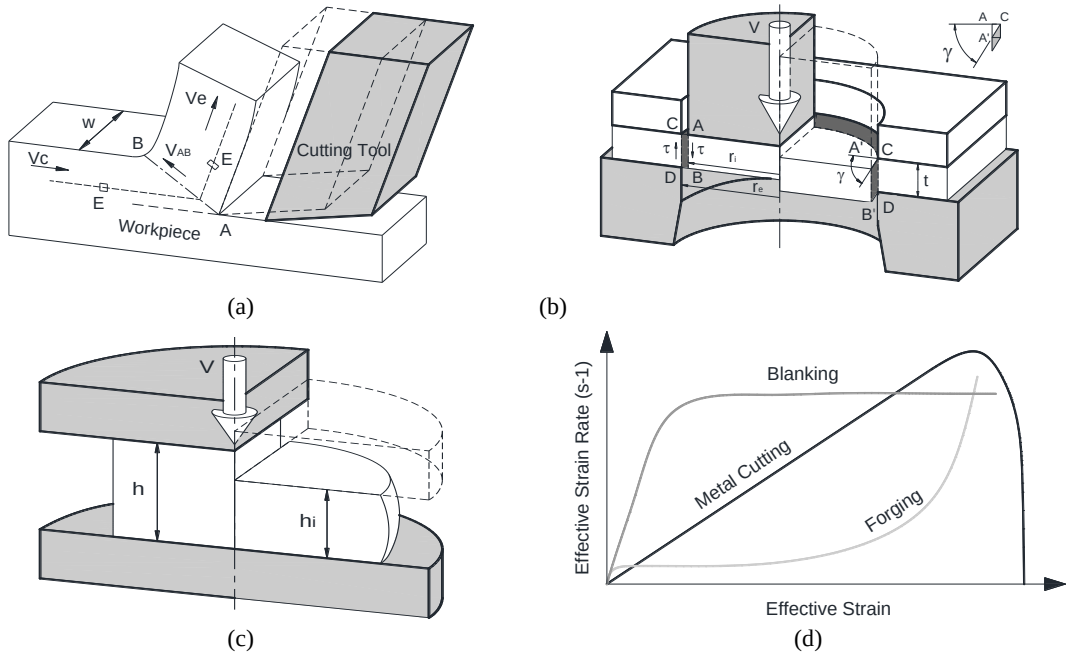

Figure 1: (a) Metal cutting, (b) blanking and (c) forging together with a schematic representation of the (d) corresponding strain-rate vs. strain loading paths.

As a result of this, mechanical characterization of materials requires a deep insight into the machines and deformation mechanics of the processes prior to choosing the most appropriate equipment and operative testing conditions [4]. Taking metal cutting as an example, the synergism between the mechanical behaviour of materials and the machine-tools requires a good understanding of the displacement-time relationship of the cutting tool and of its influence in the rate dependent variables of the process. Because strain-rate growths with the level of strain as material moves from the undeformed region to the shear plane (a very narrow plastic deformation zone around AB in Figure 1a) and decreases while material moves away from the shear plane up the rake face of the tool, the resulting strain-rate vs. strain loading path for a typical flow route (refer to E in Figure 1a) is plotted in Figure 1d.

This means that the typical strain-rate vs. strain loading paths of metal cutting are significantly different from those obtained with commercially available testing equipment for medium and high rates of loading. In case of split Hopkinson pressure bars, for example, strain-rate vs. strain loading paths are characterized by an approximately constant level of strain-rate [5], similar to that plotted for blanking in Figures 1b and 1d, while in case of drop-height testing systems the strain-rate vs. strain loading paths are similar to that of forging (Figures 1c and 1d).

The abovementioned difficulties in obtaining the flow curves at appropriate rates of loading and the aforesaid synergism between material testing and real manufacturing conditions, justify the following two-fold objective of this paper; (i) the development of an innovative cam-driven electromagnetic machine for the compression testing of materials under high rates of loading and (ii) the identification of new testing methodologies based on the selection of the strain-rate vs. strain loading paths that can easily and effectively replicate the strain-rate vs. strain loading paths found in real manufacturing.

2. Experimental work

This section presents a brief description of the innovative cam-driven electromagnetic machine, followed by the electromagnetic press and, at last, the experimental workplan.

2.1. Cam-driven electromagnetic machine

Figure 2 shows the utilized cam-driven electromagnetic machine. Three main groups of components can be identified; (i) basic structural parts, (ii) specific mechanical parts and (iii) specific electrical and electromagnetic parts.

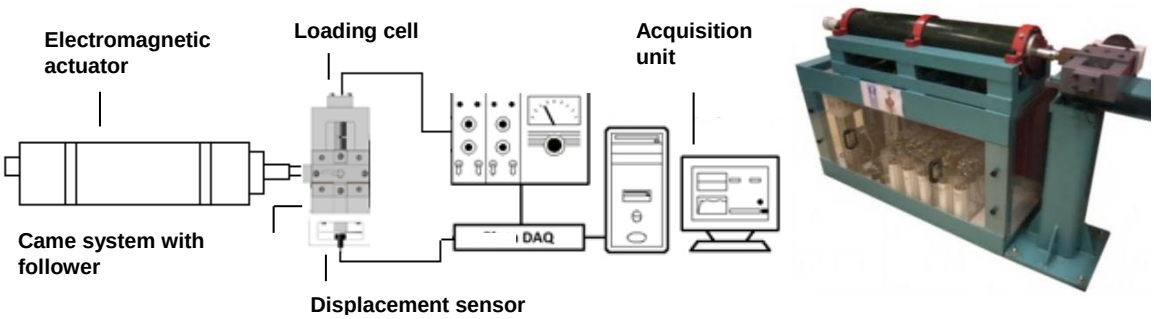

(a) (b)

Figure 2: Cam-driven electromagnetic test machine: a) Schematic representation of the test apparatus. b) Photograph of the test apparatus.

Specific mechanical parts comprise a fixed housing containing two flat compression platens, a translating cam and a follower whose design depends on the operative conditions of manufacturing to be replicated.
The compression platens are made from a cold working tool steel DIN 120WV4 hardened and tempered to 60 HRc. The translating cam and the follower are made from steel DIN 14NiCr14 and DIN 100Cr6, respectively. The clearance fit for the cam-follower system is H7/f7 (ISO) and the individual parts were manufactured in a CNC machining centre. Final manual grinding and polishing was necessary to eliminate small surface errors and imperfections that although being imperceptible to eye could cause high stress and vibrations in the cam follower. Protection of the sliding elements of the cam system was performed by means of a PTFE (Teflon added) oil based lubricant.

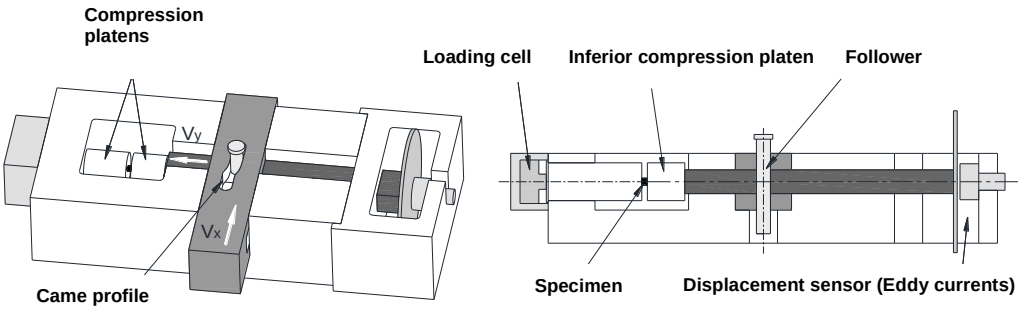

Figure 3: Schematic representation of the specific mechanical parts.

The surface contour of the cam (cam profile) is to be designed with the objective of synchronizing the performance of the testing machine with that of the machine-tool where manufacturing will take place. The follower traces the cam profile and converts horizontal movement (x) of the ram to vertical displacement (y) of the lower compression platen (Figure 2c). The conversion of movement is schematically illustrated in Figure 3.
In case of the cam shown in Figure 4b, the profile (hereafter designated as 'logistic profile') is characterized by an entry dwell followed by a rise contour and a final dwell towards the uppermost profile of the cam. The vertical displacement y of the follower as a function of the horizontal displacement x of the ram is depicted in Figure 4c.
The velocity v_y of the follower is directly related to the first derivative of the displacement curve because the velocity of the ram v_x is approximately constant in the working region of the cam follower (v_x^{avg} =10 m/s), refer to the region located in-between the dashed vertical lines in Figure 4d), $v_y = v_x^{avg} \frac{dy}{dx}$

The leftmost region in Figure 4d, characterized by a sharp increase in the velocity of the ram, results from the initial acceleration due to the pressure generated by the coils inside the electromagnetic actuator. There is no vertical movement of the cam follower along this region and, therefore, there is no compression of the upset test specimen. The rightmost region in Figure 4d unveils part of the deceleration of the ram after the follower has reached the uppermost profile of the cam. Again, there is no compression of the upset test specimen along this region.
As a result of this, the vertical movement of the cam follower leading to upset compression only takes place at the region placed in-between the dashed vertical lines in Figure 4d, hereafter named as the

'working region of the cam profile'. This justifies the reason why subsequent figures showing the displacement of the ram as the horizontal axis (x-axis) are frequently limited to the working region of the cam profile.

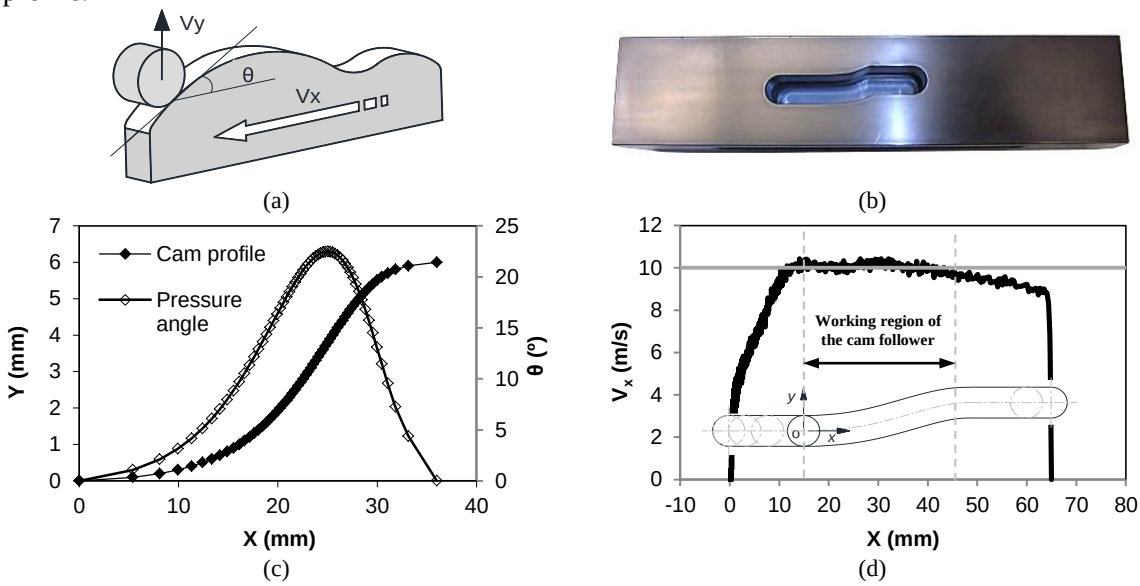

Figure 4: (a) Schematic representation of the cam profile and follower, (b) photograph of the logistic cam, (c) cam profile and pressure angle and (d) velocity of the ram v_x^{avg} =10 m/s in the working region of the cam follower.

The acceleration a_y of the cam follower is computed from the variation in the velocity v_y (assuming the above mentioned approximation of v_x) and the kinematic analysis of the follower shown in Figure 5a allows us to conclude that the cam utilized in the experiments provides the maximum velocity at the point of inflection located near the maximum slope of the cam profile.

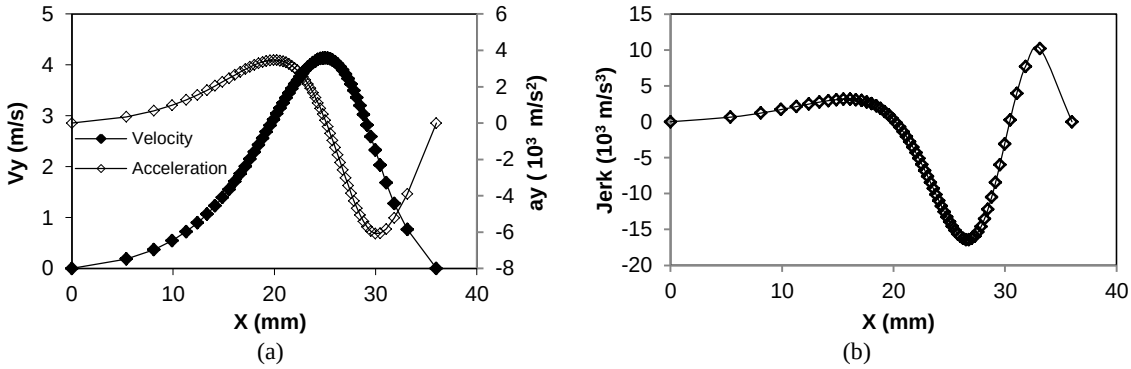

Figure 5: (a) Velocity and acceleration of the follower and (b) jerk in the working region of the cam-driven electromagnetic testing machine equipped with a logistic cam.

Acceleration is approximately constant at the entry dwell of the cam profile and presents an abrupt change from positive and to negative values at the midpoint. Along the entry dwell of the cam, jerk is approximately null (Figure 5b).

The small values of acceleration at the entry dwell of the logistic cam profile combined with the fact that pressure angles θ of the follower are kept below 30º [6] (θ^{max} =22.5º, Figure 4c), help keeping inertia forces at a small level and justify the reason why the proposed testing equipment worked smoothly without shocks and vibrations while performing material testing at high rates of loading.

The logistic cam profile allows replicating material flow conditions in conditions similar to those found in metal cutting processes [5]. However, because the cam system is flexible and its profile depends on the operative conditions to be replicated, it is easy to change the kinematics of the proposed equipment in order to replicate another manufacturing process, machine-tool or material testing equipment. For instance, replacing the logistic cam by a 'root type cam' allows the machine to replicate the kinematics of a split Hopkinson pressure bar (Figure 6).

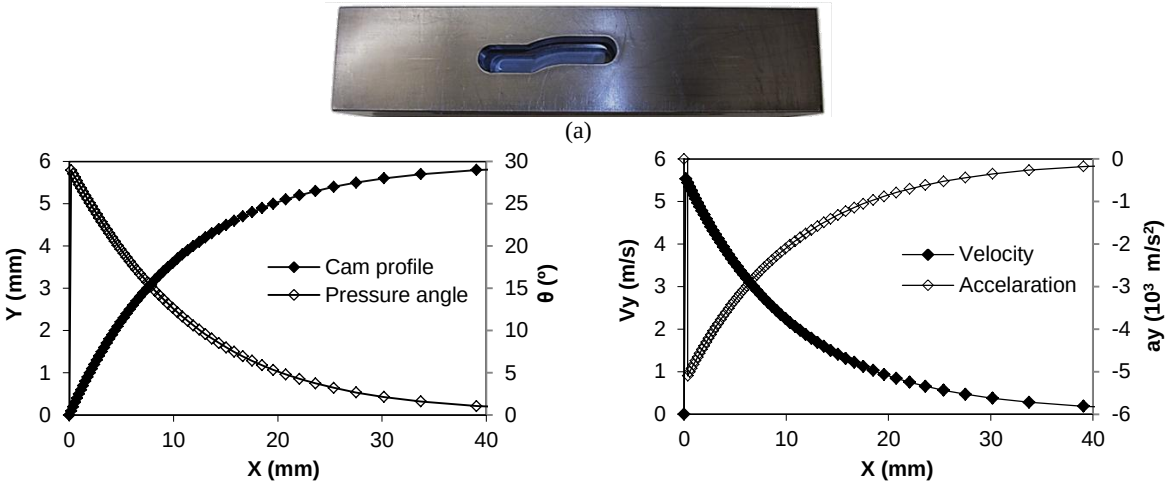

Figure 6: (a) Photograph of the root type cam, (b) cam profile and pressure angle and (c) velocity and acceleration of the follower in the working region of the cam-driven electromagnetic testing machine equipped with a root type cam.

2.2. Electromagnetic press

An electromagnetic press equipped with a specific designed tool was utilized for the fracture characterization tests (in mode II). The experimental apparatus is presented on Figure 7.

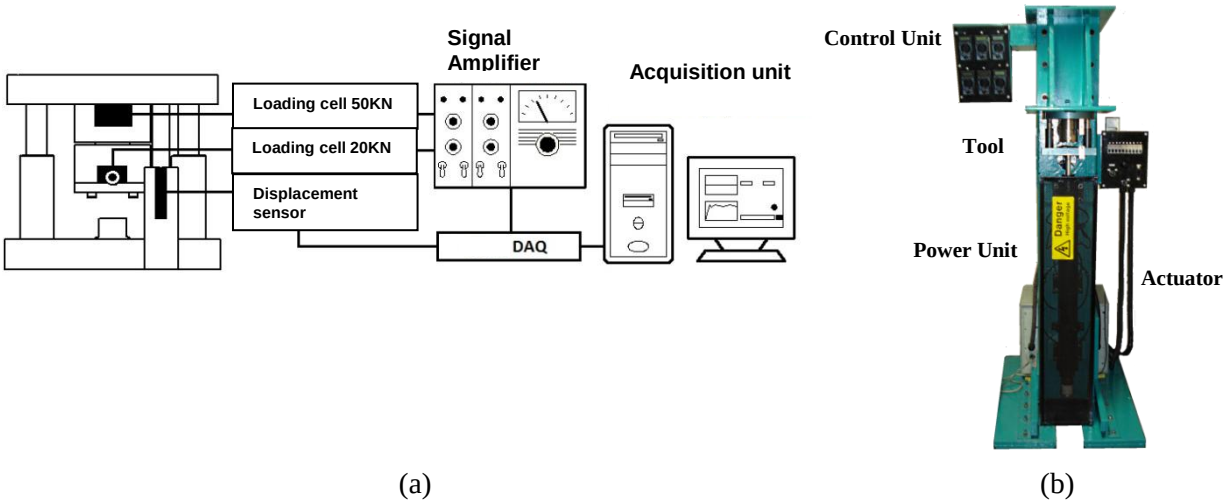

Figure 7: a) Schematic representation of the test apparatus for fracture characterization and the b) Photograph of the utilized electromagnetic press

2.3. Experimental work plan

The stress-strain curve of Aluminium AA1050-O was obtained by means of compression tests on cylindrical specimens with 6 mm diameter and 6 mm height. Both logistic and root type cam profiles were utilized (Table 1). The quasi-static conditions were included as a reference.

Case	Testing Conditions	Vx	Case	Testing Conditions	Vx
1	Quasi-static	0.01	7	Root type cam profile	3.5
2	Logistic cam profile	4	8	Root type cam profile	7
3	Logistic cam profile	3.9	9	Root type cam profile	10.4
4	Logistic cam profile	5.8	10	Root type cam profile	14
5	Logistic cam profile	7.8	11	Root type cam profile	17.5
6	Logistic cam profile	9.2			

Table 1: The plan of experiments for the mechanical characterization

In the case of fracture characterization, the specimens were obtained through conventional milling, followed by electro-discharge machining. The geometry and dimensions of the specimens are presented in Figure 8.

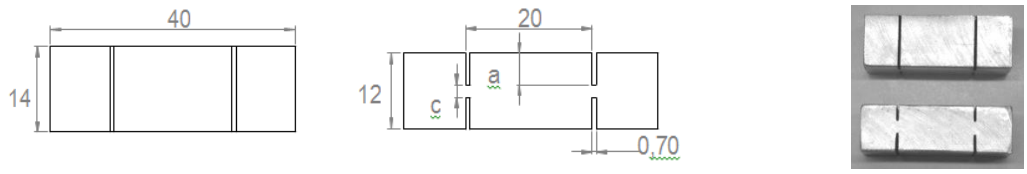

(a) (b)

Figure 8: Specimens used in fracture tests. a) Specimen dimension mm, b) Specimen Photograph

Table 2 presents the set of experiments for the fracture characterization with null normal stress, at different testing velocities. The table repeats for others set of experiments with different applied normal stresses of 30 MPa and 60 MPa.

Range of thickness c (mm)	Test velocity (m/s)		
	Quasi-static	2	3
0 – 1,5	1 e 2	6 e 7	12 e 13
1,5 – 2,5	3 e 4	8 e 9	14 e 15
2,5 – 3,5	4 e 5	10 e 11	16 e 17
Normal stress (MPa)	0		

Table 2: The plan of experiments for the fracture characterization.

3. Results and discussion

The following sections present the results of the extensive experimental work developed as mentioned on the previous section. This section can be divided in two parts: the first one, describe the mechanical characterization of the Aluminium AA1050-O, utilizing the innovative cam-driven electromagnetic machine; the second part is focused on the fracture characterization.

31. Mechanical characterization

Figure 9 shows the variation of force with displacement obtained from test cases 3 and 8 in Table 1. Results show that on contrary to root type cam profiles (and split Hopkinson pressure bars), there are no 'saw tooth' oscillations when using a logistic cam profile (case 3). This is attributed to a smooth transition between the entry dwell and the profile of the cam and to a low value of the maximum pressure angle (θ^{max} = 22.5º, Figure 4c).

The oscillations in the root type cam profile are attributed to inertia forces and stress wave propagation under impact loading as well as to an initial value of the maximum pressure angle very close to 30º (θ^{max} = 28º, Figure 5b).

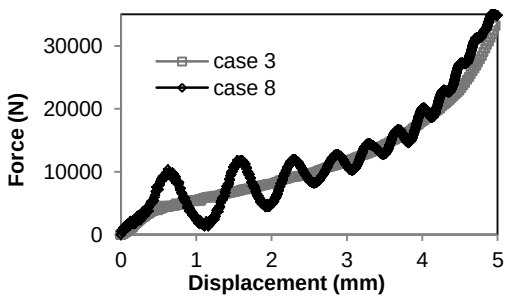

Figure 9: Experimental evolution of the force vs. displacement for logistic and root type cam profiles.

The experimental strain-rate vs. strain loading paths for the selected testing conditions performed with the cam-driven electromagnetic testing machine equipped with a logistic cam profile are plotted in Figure 10a.

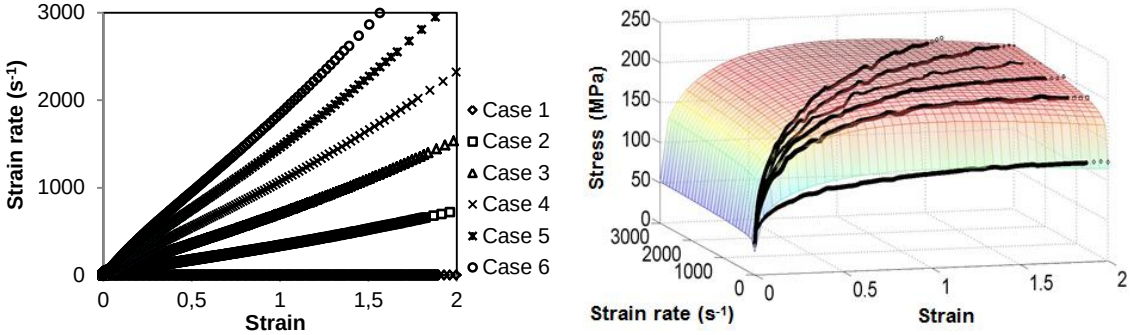

(a) (b)

Figure 10: Mechanical testing of Aluminium AA1050-O using a logistic cam. (a) Strain-rate vs. strain loading paths. (b) Material stress response with respect to strain and strain-rate (experimental data and fitting).

The three-dimensional flow surface plotted in Figure 10b in which stress, strain and strain-rate are the leading axis results from fitting experimental data to the following mathematical material model that was developed by the authors [5],

$$\sigma = \left(A + e^{m\varepsilon}\varepsilon^{n}\right)\left(B + C\,ln\left[D + \dot{\varepsilon}\right]\right) \tag{1}$$

where, the constants A, B, C, D, m and n are to be determined from experimental data. The model given by equation (1) is appropriate for cold forming operating conditions and includes well-known material models such as Ludwik-Holloman, Voce and Johnson-Cook (isothermal), among others, as special cases. Another advantage of this model is the ability for exhibiting material flow softening at high values of strain. Flow softening is responsible for diminishing the resistance to plastic deformation due to rearrangement of dislocations under dynamic recrystallization and is known to cause a significant influence in the deformation mechanics of metal cutting, namely chip formation [7].

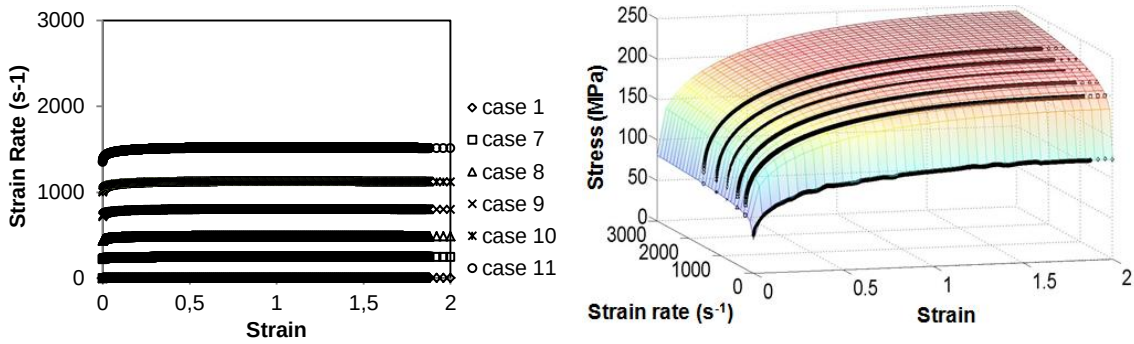

(a) (b)

Figure 11: Mechanical testing of Aluminium AA1050-O using a root type cam. (a) Strain-rate vs. strain loading paths. (b) Material stress response with respect to strain and strain-rate (experimental data and fitting).

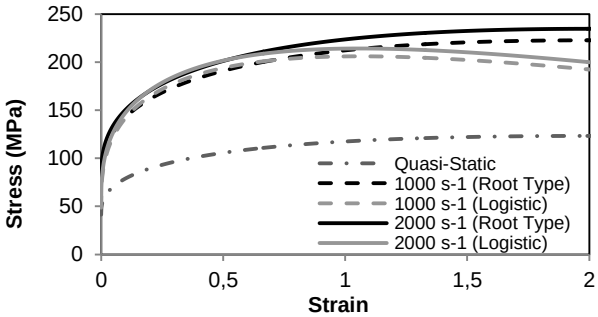

Figure 10: Experimental stress–strain curves after mathematical fitting for different values of strain-rate.

Figure 11a provides similar results for the root type cam. As seen, the strain-rate vs. strain loading paths obtained with this type of cam are near horizontal lines and similar to those commonly attained with Hopkinson pressure bars. The three-dimensional flow surface resulting from these experiments is plotted

in Figure 11b. The differences between the flow surfaces obtained from material testing with logistic and root type cams are made clear by analysing a selection of intersections of the three-dimensional flow surfaces with constant strain-rate planes ($\dot{\bar{\varepsilon}} = Cte$). The flow curves resulting from these intersections are plotted in Figure 10 and indicate that major differences are due to flow softening in close agreement with the aforementioned capability of the logistic cam profile to model metal cutting conditions.

3.2. Fracture characterization

The cracks initiate and grow when a required energy is applied. The common procedure in fracture mechanics is to quantify the value of this critical energy by calculating the total energy W, from the following equation,

$$W_{Exp.} = \int_0^{x_{F_{Máx}}} F_{Exp.}\, dx \tag{2}$$

Fracture toughness, R, is the energy required for the formation of new surfaces, is defined per unit of area confined by the length of the ligament between notches, [9].

$$R = \lim_{c\to 0}(w) = \lim_{c\to 0}\left(\frac{W_{Exp.}}{A}\right) = \lim_{c\to 0}\left(\frac{W_{Exp.}}{p\,.\,c}\right) \tag{3}$$

These experiments were designed for determining the evolution of the force with displacement for different velocities (quasi-static, 2m/s and 3m/s) and of the ligament remaining between the starting cracks (Figure 11).

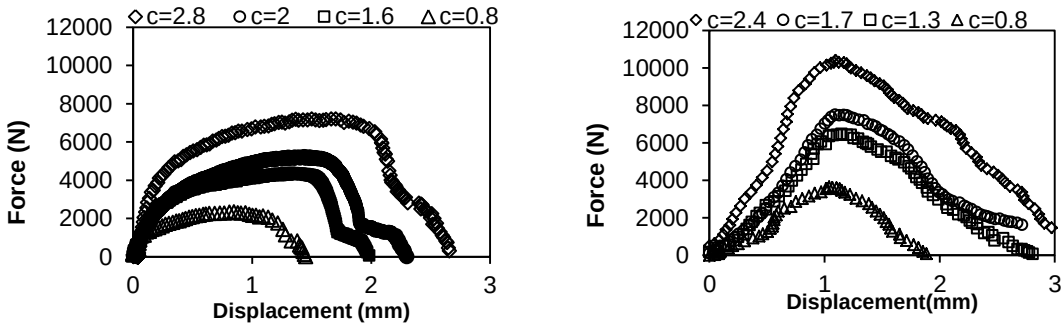

(a) (b)

Figura 11: Evolution of the force with the displacement for different values of ligament between notches for: a) quasi-static and b) v = 3m/s

For the determination of the value of fracture toughness R, tests with different ligament between notches were conducted, followed by the extrapolation of the experimental values for the limit as its values tend to zero. The results are presented in Figure 12 a), and its evolution with the applied normal stress with different test velocities is presented in Figure 12 b).

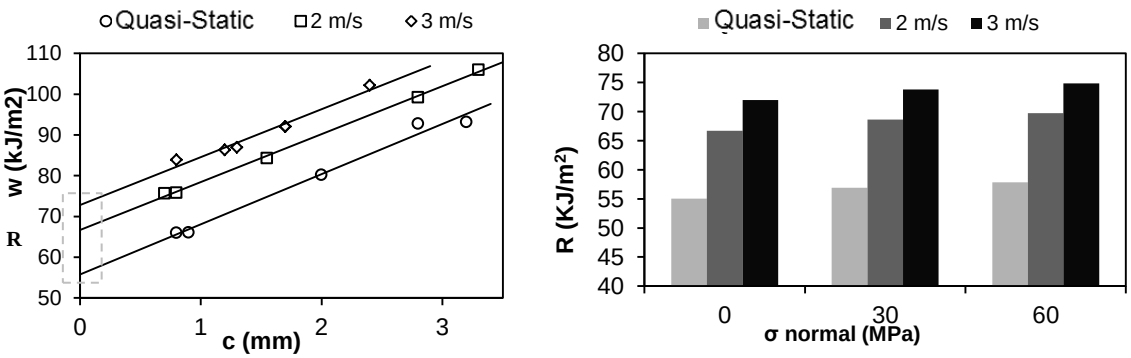

(a) (b)

Figure 12 a) Procedure for calculating R without applied normal stress. b) Evolution of R with different normal stresses and test velocities.

Figure 4.8 show that fracture toughness increases with the test velocity. In the other hand, it is also verified for all the tested velocities that, the value of the energy per area increases with the increase of the value of the ligament between notches. Figure 12 b) shows that the value of the fracture toughness increases with test velocity and the applied normal stress.

Another procedure for analyzing the experimental results were utilized, for determining the energy per volume U, which is require for the formation of new surfaces. This value results in the subtraction of the total energy from an experimental test with the supposed theoretical value (from plastic deformation). However, there is no generalized consensus of the physical fundamentals behind this methodology, the present research work demonstrates that this technique presents quite satisfactory results.

$$U = \frac{W_{exp} - W_{plást.}}{V_{entalhe}} \tag{4}$$

The theoretical value of the required energy for the plastic deformation of the material was calculated from finite element methods (FEM), by in-house computer program I-FORM. Figure 13 presents the obtained values for U for different ligament between notches and test velocities.

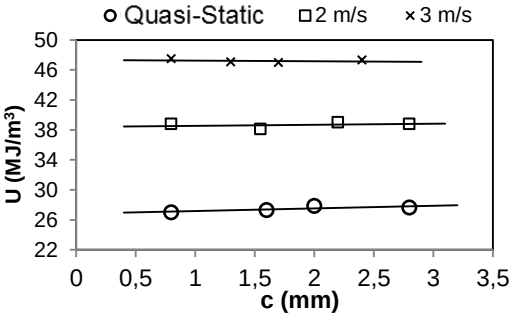

Figure 13: Evolution of the energy per volume U with the ligament between notches and test velocity.

It can be observed that U remains almost constant with the ligament between notches c, for a specific test velocity. This result validates indirectly, the supposed plastic deformation is limited for the material near the notches.

One of the most important parameter to preview in the modelling of this test is the maximum shear force By taken into account the as the total energy is the sum of several parts, it is expected that the maximum shear force can be also obtained by the sum of the plastic deformation, formation of new surfaces and the friction between tool and specimen [8]..

$$F_{max} = F_{plast.} + F_{fract.} + F_{frict} \tag{5}$$

As this type of test does not present relative movement between tool and specimen, the part of the friction can be ignored. The force required for the formation of the new surfaces is obtained by calculating the specific R and U as showed in Equation 7:

$$F_{fract.} = R.p \quad \text{or } F_{fract.} = U.p.c \tag{6}$$

For the determination of the force required for the plastic deformation of the material F_{plast}, it is admitted that the separation of the material is caused by the shear stresses and the maximum shear force is proportional to maximum shear stress $\tau_{Máx.}$ across the cutting perimeter of the specimen. It is represented in Equation 8, where the maximum shear stress is replaced by the value result from the Von Mises plasticity criterion $\tau_{máx} = \sigma_e/\sqrt{3}$ [10].

$$F_{Plast.} = \frac{1}{\sqrt{3}}\,\sigma_e\ p\ h \tag{7}$$

These force values associated to the plastic deformation of the material were alternatively counted by the numeric simulation with FEM, by I-FORM. The differences obtained with these two methodologies are almost inexistent as can be observed in Figure 13.

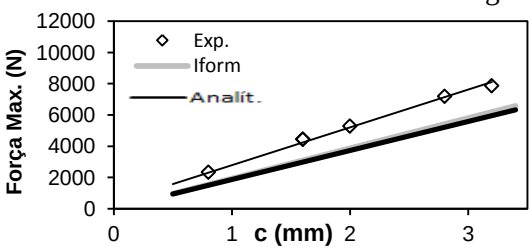

a)

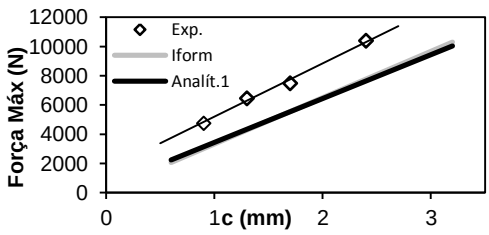

b)

Figure 13: Comparison between the experimental results, theoretical and FEM results at a) quasi-static and b) v = 3m/s conditions.

The evaluation of the determination of the maximum shear force based on the plasticity and fracture analysis was conducted by comparing the experimental results with the sum of the force due to plastic deformation and the force that was required for the formation of new surfaces (obtained from R and the energy per volume U). The results are presented in Figure 14

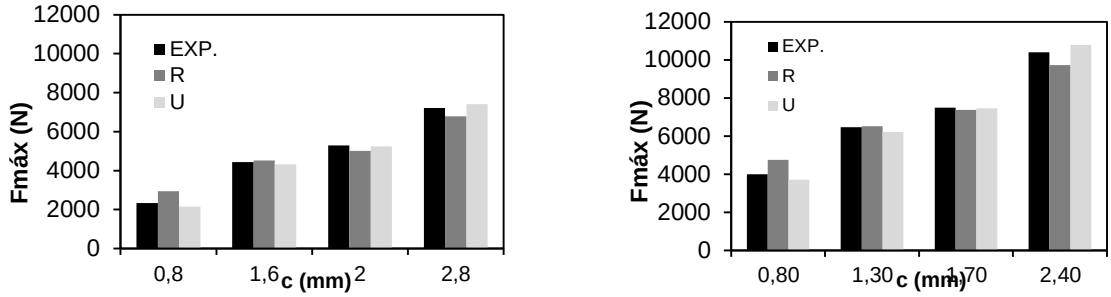

Figure 14: Experimental values and the calculated maximum shear force as a function of the value of ligament between notches at a) quasi-static and b) 3 m/s.

5. Conclusions

The experimental results shows that the cam-driven electromagnetic testing machine is capable of operating across a broad range of operative conditions found in real manufacturing processes. The results also show that the proposed machine equipped with a logistic cam is capable of diminishing 'saw tooth' oscillations in the experimental recordings of force that are typical of split Hopkinson pressure bars and root type cam profiles. Moreover logistic cam profiles in conjunction with the proposed material model are able to successfully model flow softening that is commonly found in metal cutting applications. The present work also demonstrates the impact of the velocity profiles on the material's flow curve.

The experimental results also points out the important role of the ductile fracture mechanics in the manufacturing processes where the formation of new surfaces takes place. It can be concluded that the value of the fracture toughness R depends on the strain rate, and not the value of the ligament remaining between the starting cracks (for the same strain rate). It also shows that the normal stress shows little influence on the value of R, for the tested strain-rate. In conclusion, the experimental results of the present research work are particularly important for the modelling of manufacturing processes where the formation of new surfaces takes place.

References

[1] Banabic D., Bunge H.-J., Pöhlandt K., Tekkaya A. E., Formability of metallic materials, Springer-Verlag, Berlin, 2000.

[2] Silva C. M. A., Rosa P. A. R. and Martins P. A. F., Mechanical characterization of materials for bulkf using a drop weight testing machine, Journal of Mechanical Engineering Science, 2010, 224, p. 1795-1804.

[3] Guo Y., Saldana C., Mann J. B., Saoubi R. M., Chandrasek S, Deformation and microstructure in machining, Advanced Materials Research, 2011, 223, p.325-331.

[4] Field J. E., Walley S. M., Proud W. G., Goldrein H. T., Siviour C. R., Review of experimental techniques for high rate deformation and shock studies, International Journal of Impact Engineering, 2004, 30, p. 725–775.

[5] Silva C. M. A., Rosa P. A. R., Martins P. A. F., Electromagnetic cam driven compression testing equipment", Experimental Mechanics, 2011 (on-line first).

[6] Rothbart H. A., Cam design handbook. McGraw Hill, New York, 2004.

[7] Sima M., Özel T., Modified material constitutive models for serrated chip formation simulations and experimental validation in machining of titanium alloy Ti-6Al-4V. International Journal of Machine Tools and Manufacture, 2010, 50, p. 943–960.

[8] Turner CE., "A re-assessment of ductile tearing resistance (Part I and II)". Fracture Behaviour and Design of Materials and Structures. Proc ECF 8, vol. II. p. 933–49. and p. 951–68, 1990.

[9] Atkins A. G., "Modelling metal cutting using modern ductile fracture mechanics: quantitative explanations for some longstanding problems", *Int. J. Mech. Sci.*, 45: 373-396, 2003.

[10] Rodrigues J.M.C. and Martins P.A.F., "Tecnologia da deformação plástica, Vol. I. Fundamentos teóricos", Escolar Editora, Portugal, (2005).